

# Immunogenicity of different stressed IgG monoclonal antibody formulations in immune tolerant transgenic mice

Vasco Filipe,<sup>1,2</sup> Wim Jiskoot,<sup>1,\*</sup> Abdul Hafid Basmeh,<sup>2</sup> Andhyk Halim,<sup>2</sup> Huub Schellekens<sup>2</sup> and Vera Brinks<sup>2</sup>

<sup>1</sup>Division of Drug Delivery Technology; Leiden/Amsterdam Center for Drug Research; Leiden University; Leiden, The Netherlands; <sup>2</sup>Department of Pharmaceutics; Utrecht Institute for Pharmaceutical Sciences (UIPS); Utrecht University; Utrecht, The Netherlands

**Keywords:** IgG, accelerated stress conditions, protein aggregates, immunogenicity, transgenic mice

The presence of protein aggregates in biopharmaceutical formulations is of great concern for safety and efficacy reasons. The aim of this study was to correlate the type and amount of IgG monoclonal antibody aggregates with their immunogenic potential. IgG degradation was obtained by freeze-thawing cycles, pH-shift cycles, heating, shaking and metal-catalyzed oxidation. The size, amount, morphology and type of intermolecular bonds of aggregates, as well as structural changes and epitope integrity were characterized. These formulations were injected in mice transgenic (TG) for human genes for Ig heavy and light chains and their non-transgenic (NTG) counterparts. Anti-drug antibody (ADA) titers were determined by bridging ELISA. Both unstressed IgG and freeze-thawed formulation did not induce measurable ADA levels. A mild antibody response was obtained in a fairly small percentage of mice, when injected with shaken, pH-shifted and heated formulations. The metal-catalyzed oxidized IgG formulation was the most immunogenic one, in both ADA titers and number of responders. The overall titers of NTG responders were significantly higher than the ones produced by TG mice, whereas there was no significant difference between the overall number of TG and NTG responders. This study reinforces the important role of protein aggregates on immunogenicity of therapeutic proteins and provides new insight into the immunogenic potential of different types of IgG aggregates. The results indicate that the quality of the IgG aggregates has more impact on the development of an immune response than their quantity or size.

## Introduction

Monoclonal antibodies (mAbs) are used to treat a wide range of diseases and are currently the fastest growing drug category.<sup>1</sup> However, a major concern associated with the use of mAbs, and nearly all other therapeutic proteins, is that their repeated administration to patients often leads to the induction of anti-drug antibodies (ADAs). The development of ADAs in patients may influence pharmacokinetics (PK) and significantly lower efficacy, as has been observed, e.g., for anti-tumor necrosis factor (TNF) antibodies used for the treatment of rheumatoid arthritis.<sup>2,3</sup> In some cases, the formation of ADAs leads to severe adverse effects and life-threatening situations.<sup>4</sup>

Among the factors playing a role in immunogenicity, the presence of aggregates in formulations has been put forward as a major concern.<sup>5</sup> Several studies have suggested that formulations with a high amount of aggregates tend to be more immunogenic.<sup>6,7</sup> Thus, the presence of aggregates in biopharmaceutical products has become a main concern for the pharmaceutical industry and regulatory agencies, but little is known about the nature of the aggregate species responsible for immune reactions or the immune mechanisms involved. Recognition and processing of

aggregates has been reported to be accomplished through non-specific uptake by APCs and specific uptake by B cells.<sup>8-10</sup> Protein aggregates may expose neo-epitopes, cryptic epitopes or repetitive epitopes, and these intrinsic differences may determine the mechanism by which they trigger the immune system.<sup>11</sup>

The characterization of protein aggregates is complex and requires the use of many different analytical techniques.<sup>12,13</sup> Until recently, the presence of visible aggregates (> 100  $\mu\text{m}$ ) and relatively large (> 10  $\mu\text{m}$ ) subvisible particles in parenteral formulations had been the main concern for adverse reactions, whereas subvisible aggregates < 10  $\mu\text{m}$  and submicron (< 1  $\mu\text{m}$ ) aggregates had been largely overlooked. It seems increasingly likely, however, that the latter type of aggregates is involved in the development of immunogenicity.<sup>14</sup> Until only a few years ago, subvisible aggregates posed a particular analytical challenge, mostly due to the lack of suitable techniques for their size range. This is now changing with the continuing development of new analytical techniques such as nanoparticle tracking analysis (NTA), flow microscopy, Taylor dispersion analysis and the revival of Coulter counter methodology.<sup>15-20</sup>

Several predictive models for immunogenicity of therapeutic proteins have been suggested. The available methods to predict

\*Correspondence to: Wim Jiskoot; Email: w.jiskoot@lacdr.leidenuniv.nl  
Submitted: 07/24/12; Revised: 08/30/12; Accepted: 09/03/12  
<http://dx.doi.org/10.4161/mabs.22066>

**Table 1.** AUC percentages from SEC-UV analysis and particles/ml of NTA and LO measurements of unstressed and stressed IgG formulations

	SEC-UV (%)				Total aggregation	NTA	LO
	Fragments	Monomers	Oligomers	Relative recovery		Aggregates/ml	Aggregates/ml
Unst	0.7	98.0	1.2	100	1	$1 \times 10^7$	$3.0 \times 10^3$
FT	0.5	98.0	1.4	94	7	$4 \times 10^7$	$8.9 \times 10^4$
pH shift	1.7	49.8	48.5	63	67	$3 \times 10^9$	$1.7 \times 10^5$
Heat	1.0	64.2	34.8	94	39	$1 \times 10^{10}$	$1.6 \times 10^4$
Shake	2.0	96.6	1.4	12	88	$7 \times 10^7$	$4.1 \times 10^5$
Met Ox	35.8	46.6	17.6	N/A	N/A	$7 \times 10^7$	$1.3 \times 10^4$

Abbreviations and notes: Unst, unstressed; FT, freeze-thawed; Met Ox, metal-catalyzed oxidized; N/A, not available (see text). Percentages of fragments, monomers and oligomers refer to the total AUC of each sample. Relative recovery refers to total AUC of each sample compared with total AUC of the unstressed one. Total aggregation refers to the sum of unrecovered protein plus recovered oligomers.

immunogenicity involve in silico, in vitro and in vivo approaches. In silico and in vitro techniques are mostly based on the aptitude of proteins to actively interact with immune or innate cells.<sup>21,22</sup> Even though some approaches may take into consideration protein aggregates, at the moment in silico techniques do not seem to be mature enough for predicting aggregate-related immunogenicity.<sup>11</sup> In vitro techniques seem to have more predictive potential in this field and are currently being explored for studying formulation-related immunogenicity, including the role of aggregates.<sup>10,23</sup> In contrast, methods for in vivo prediction include the entire immune machinery and environment necessary to better simulate the extremely complex scenario that results in complete immune responses, especially when protein aggregates are involved. Thus, currently the use of animal models to predict immunogenicity in vivo seems to be the most promising approach to predict aggregate-related ADA responses.<sup>6,24-26</sup>

An advantage of in vivo assessment of immunogenicity is that the complex interplay between different aspects of the immune system (i.e., immune cells, cytokines) is accounted for. This is of importance when studying the immunogenicity of aggregates, in which the underlying immune mechanisms leading to antibody formation are mostly unknown. The vast majority of proteins used for therapeutic purposes in humans are, however, foreign to animals. As a consequence, these mice normally develop a classical immune response against a foreign protein when exposed to human protein drugs, which is not necessarily the type of response observed in patients. Therefore, to circumvent this problem, transgenic animal models that express the human protein of interest have been developed and should render a good model for immunogenicity testing.<sup>27</sup> These mice are, like humans, immune tolerant to a specific human protein and provide the opportunity to study the factors that underlie immunogenicity of therapeutic proteins, including breaking/circumventing of immune tolerance.

The risk that aggregates pose for immunogenicity has been studied for a number of different therapeutic proteins in transgenic mice,<sup>28-30</sup> but the immunogenicity of mAbs using an appropriate TG mouse model has never been systematically studied. In this work, a human mAb of the IgG<sub>1</sub> subclass was aggregated by different pharmaceutically relevant stress factors: freeze-thawing cycles, pH-shift cycles, heating, shaking and metal-catalyzed

oxidation. The resulting formulations were characterized by different complementary analytical methods. These samples were then injected in a TG mouse strain carrying human Ig genes, the five-feature translocus mice,<sup>31</sup> for in vivo immunogenicity testing.

## Results

**Characterization of stressed IgG formulations.** *Size distribution of protein aggregates.* Size exclusion chromatography (SEC) was used to separate and quantify monomers and small oligomers present in unstressed and stressed formulations. The detection was made by UV absorption at 280 nm and by multiple angle laser light scattering (MALLS), and the molar mass of each peak was estimated (Fig. 1A and B). The area under the curve (AUC) percentages of fragments, monomers, oligomers and relative protein recovery were calculated based on the UV signal; these are summarized in Table 1.

Nanoparticle tracking analysis (NTA) and light obscuration (LO) were used to analyze the size distribution of aggregates that were above the size detection limit of SEC, i.e., submicron and micron-sized aggregates (Fig. 1C and D). NTA is an emerging technique that enables the visualization, sizing and quantification of particles in the submicron range (ca. 40–1000 nm). LO particle counting is a technique that can count and measure the size of micron-sized particles (1–200  $\mu\text{m}$ ). The total amount of aggregates per ml measured by these techniques is shown in Table 1.

*Size exclusion chromatography (SEC).* It is clear from Figure 1A and B that all stressed IgG samples contained aggregates, detectable not only by the presence of oligomer peaks but also by monomer peak loss compared with the unstressed formulation. Among the stress factors applied, freeze-thawing induced the smallest percentage of aggregation since this sample only differed from the unstressed formulation by having a slightly smaller amount of monomer.

The pH-shift stressed sample was the one with the highest percentage of oligomers (48.5%) and had the second highest total aggregation percentage (67%). The heat stressed formulation also contained a high percentage of oligomers (ca. 34.8%). The presence of larger oligomers can be clearly observed in the MALLS

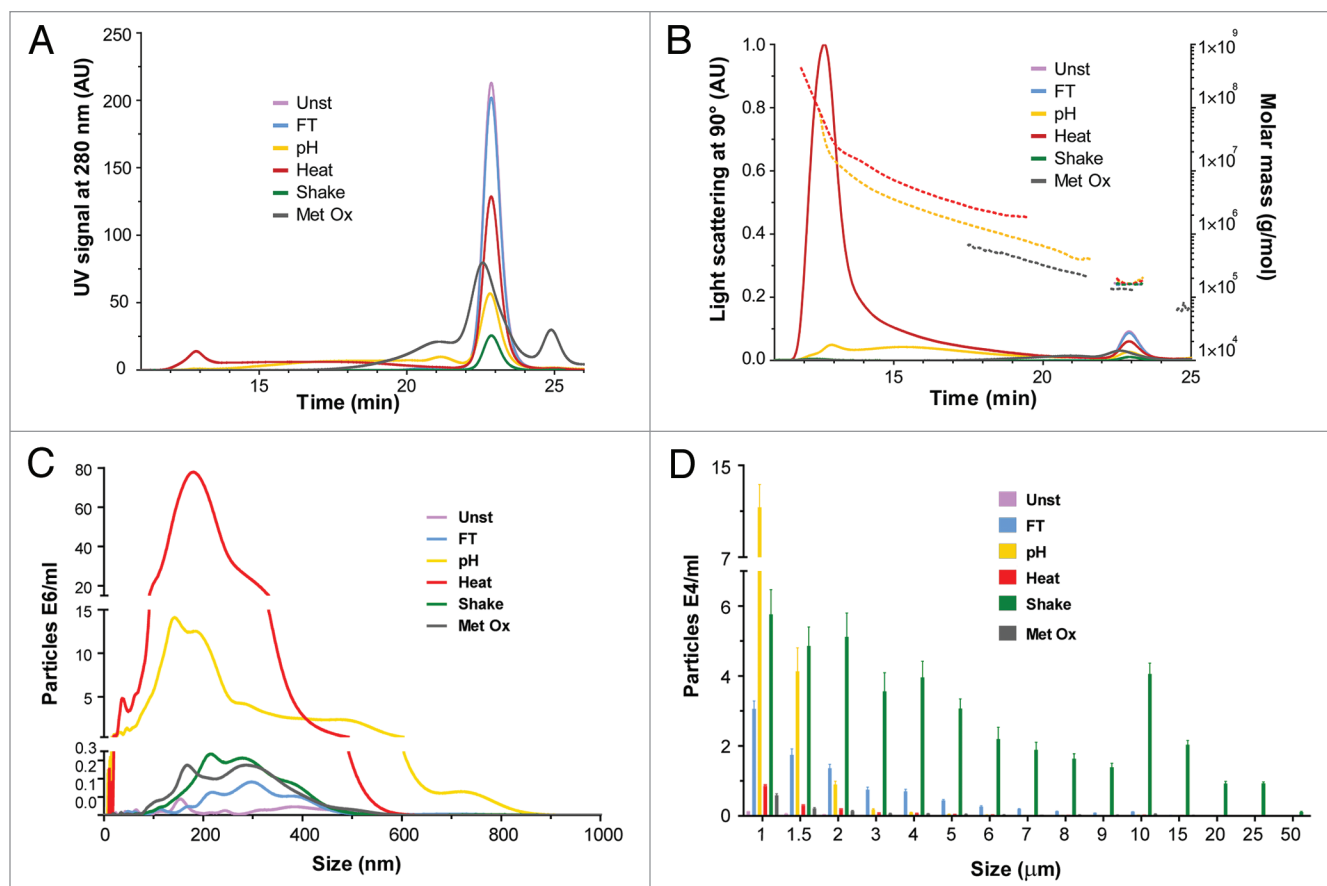


**Figure 1.** Size distribution of unstressed (Unst), freeze-thawed (FT), pH-shifted (pH), heated (Heat), shaken (Shake) and metal-catalyzed oxidized (Metal Ox) IgG formulations: (A) SEC with UV detection at 280 nm; (B) SEC with MALLS detection and the estimated molar mass of each peak; (C) submicron particles (determined by NTA), (D) micron-sized particles (determined by LO).

chromatogram (Fig. 1B). pH-shift stress induced the formation of a large amount of dimers, trimers and other small oligomers, whereas heat stress induced mostly the formation of larger oligomers. The shaken stressed sample had the highest total aggregation percentage (88%); however, practically no oligomer peaks were detected for this sample, indicating that most of the aggregates were too large to be analyzed by SEC.

Metal-catalyzed oxidation induced the formation of a large amount of fragments (35.8%) that have a distinct peak eluting at 25 min in the chromatogram of Figure 1A. This fragmentation seems to have been accompanied by oligomerization of fragments or intact monomers, which led to the broadening of the monomer peak. This broad peak had an AUC larger than the one of the unstressed formulation, which resulted in an improbable relative recovery (> 100%). It is possible that the oxidation process induced the formation of oxidized species or amino acids with higher extinction coefficients at 280 nm, which would have resulted in larger AUCs. In any case, the relative recovery and total aggregation percentages of oxidized samples could not be accurately calculated.

The estimated molar mass of the monomer peak of all but the oxidized sample was about  $1.5 \times 10^5$  g/mol, which is consistent with the expected value for IgG. Monomers of the oxidized

sample had an estimated molar mass of  $1.3 \times 10^5$  g/mol. This may have to do with the contribution of fragmented monomers or oligomerized fragments to the monomer peak. The oligomers of the oxidized sample also had a lower estimated molar mass than the ones of the pH-shift and heat stressed samples. This may have to do with a potentially higher extinction coefficient of these species (see above) compared with the oligomers of pH-shift and heat stressed samples.

**Nanoparticle Tracking Analysis (NTA).** According to NTA results (Table 1), the heated sample contained substantially more submicron aggregates than the other samples, in agreement with the trend shown by SEC. The pH shift sample also contained a considerable amount of aggregates compared with the other samples, but still 3 times lower than the heated sample.

The size average of submicron aggregates was fairly similar between the stressed samples (Fig. 1C), with exception for the pH-shift stressed sample. This sample was very polydisperse and was the only one containing a fairly high amount of submicron aggregates larger than 600 nm. For this reason, this sample was the only one analyzed with the *extended dynamic range* mode, more suitable for very polydisperse samples.<sup>17</sup> Most aggregates larger than 600 nm, however, contained multiple scattering centers, which added a rotational variable that cannot be analyzed

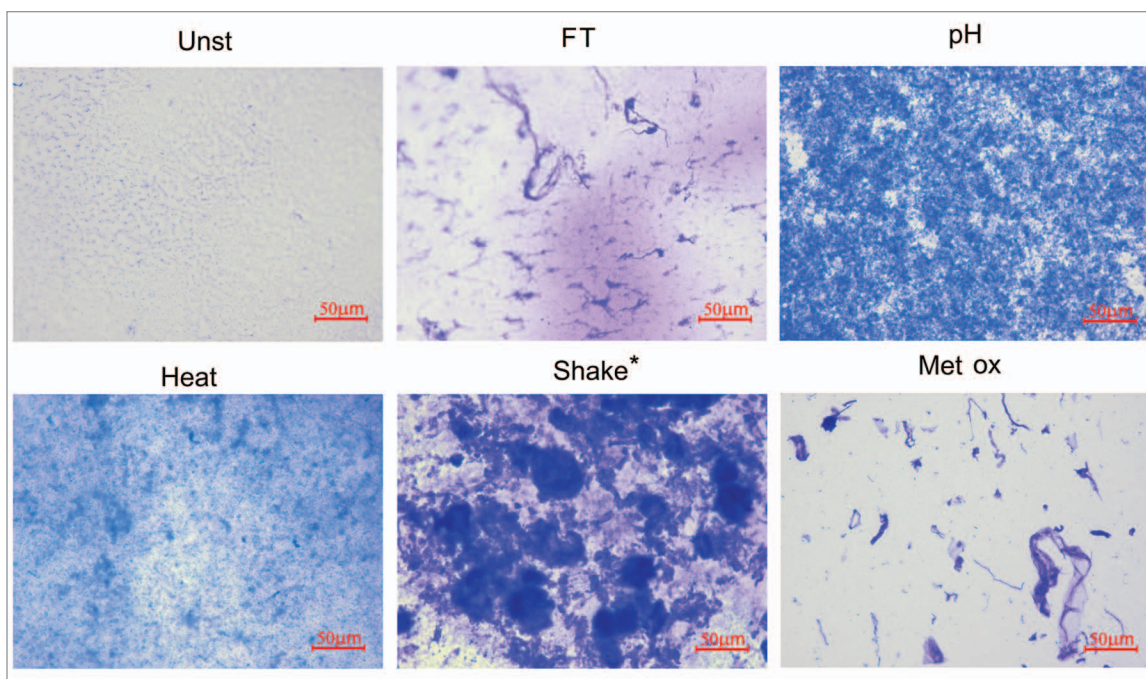


**Figure 2.** Representative microscopy images (20x amplification) of unstressed (Unst), freeze-thawed (FT), pH-shifted (pH), heated (Heat), shaken (Shake) and metal-catalyzed oxidized (Metal Ox) IgG formulations after filtration through a 0.22  $\mu\text{m}$  filter, followed by staining with Coomassie brilliant blue. \*The filtered volume used for the shaken formulation was 10 times lower than that for the other formulations due to filter blockage.

correctly by the software. Thus, the amount of large submicron aggregates in the pH-shift sample was actually higher than the one obtained by NTA.

**Light Obscuration (LO).** According to LO results, the size bin with the highest amount of particles was between 1 and 1.5  $\mu\text{m}$  for all samples (Fig. 1D). All samples presented a skewed particle size distribution with most particles being in the lower size bins, except for the shaken sample, for which the distribution was broad and multimodal. This sample also contained the highest amount of micron-sized aggregates, followed by the pH shift and then by the freeze-thawed samples.

**Filtration with Coomassie Blue staining.** To obtain information about the morphology of the subvisible aggregates in each sample, the formulations were filtered through a 0.22  $\mu\text{m}$  filter and the aggregates retained on the membrane were stained with Coomassie brilliant blue. The membranes were then analyzed with a light microscope and representative images of each sample are shown in Figure 2.

As expected, the shaken sample contained the biggest aggregates of all stressed samples. These aggregates were fairly rounded and seem to be relatively dense. Freeze-thawed micron-sized aggregates resembled loose threads with random knots. The oxidized sample showed a mixture of thread-like structures, compact irregular shapes and dense smoke-like structures. pH-shift stress induced aggregates that are numerous and relatively small, in such a way that it is impossible to describe their morphology. Heat induced aggregates were so small, when analyzed by this technique, that only a faint blue cloud with occasional dark spots can be observed. It is important to mention that this is not a quantitative technique because variable amounts of aggregates

may be removed from the membrane during staining and destaining incubation periods.

**Visual inspection.** All stressed formulations remained free of visible particles during the entire time course of the experiment, except the shake stressed sample. In this sample, very small visible particles were observed immediately after stress. Most of these precipitates remained adsorbed to the air bubbles caused by the stress, indicating a high degree of hydrophobicity of these aggregates. These air bubbles disappeared by the time of injection/analysis, when only a small white deposit was observable.

**Structural changes.** To obtain information about the overall structural changes induced by the different stresses, the formulations were analyzed by circular dichroism (CD) and bis-ANS fluorescence. From the far-UV CD region (200–250 nm), which corresponds to the peptide bond absorption, information on the secondary structure of a protein can be obtained.<sup>32</sup> The near-UV CD region (250–320 nm) reflects the environment of the aromatic amino acid side chains and therefore yields information about the tertiary structure of a protein.<sup>32</sup> Bis-ANS is a dye that fluoresces intensely only in hydrophobic microenvironments, such as exposed hydrophobic pockets of proteins, thus yielding information about the tertiary structure.<sup>33</sup> The CD and bis-ANS fluorescence results are shown in Figure 3.

**Far-UV circular dichroism (CD).** The far-UV CD spectrum (Fig. 3A) of the unstressed IgG formulation has a minimum at  $\sim 220$  nm and a maximum at 204 nm, indicative of a high  $\beta$ -sheet structure, which is typical for IgG.<sup>34,35</sup> All stressed samples showed a clear reduction of the mean residue ellipticity ( $[\theta]_{\text{MR}}$ ) at 204 nm, indicating that some changes in secondary structure occurred in all formulations. The spectrum of the heat stressed



sample was the one that most changed, with a distinctly more negative  $[\theta]_{MR}$  at 220 nm, whereas the other samples showed only marginal spectral changes at this wavelength. The spectrum of the freeze-thawed sample is the one with fewer overall changes. It may be important to note that most of the shake stress-induced aggregates were not present in this sample for this measurement, so the spectrum obtained for this sample represents mostly the remaining monomer. These aggregates severely interfered with far-UV CD measurements, mainly due to light scattering, and thus had to be spun down before these measurements.

**Near-UV circular dichroism (CD).** The near-UV CD spectrum (Fig. 3B) of the unstressed formulation has a distinctive positive peak at 295 nm (tryptophan) and a negative band in the range between 250 and 290 nm (aromatic amino acid residues and cysteine), which is typical for IgG.<sup>34,36</sup> The spectrum of the freeze-thawed formulation is shifted to more negative  $[\theta]_{MR}$  and has approximately the same shape as the unstressed sample. The spectrum of the heated sample is equally shifted, but has some shape differences, particularly from 250 to 280 nm and from 300 to 320 nm. The oxidized sample showed clear spectral changes, with reduced  $[\theta]_{MR}$  between 290 and 320 nm and significantly increased  $[\theta]_{MR}$  between 250 and 290 nm compared with the unstressed sample. The spectrum of the pH-shifted sample not only has a different shape, but is also considerably shifted to lower  $[\theta]_{MR}$ . Such pronounced changes can be attributed to light scattering effects, which can cause artifacts due to: (1) differential light scattering, arising when light falls on chiral particles of dimensions comparable to or greater than its wavelength; and (2) absorption flattening due to the high protein concentration in aggregates.<sup>32</sup> In fact, such light scattering effects were so pronounced with the shake-stressed formulation that the near-UV CD results of this sample had to be discarded.

**bis-ANS fluorescence.** As can be observed in Figure 3C, all stressed samples exhibited increased bis-ANS fluorescence compared with the unstressed formulation. The fluorescence intensity of stressed samples followed the order: heated > shaken > pH-shifted > oxidized > freeze-thawed. These results indicate that the conformational changes, already observed by CD, lead to enhanced exposure of hydrophobic patches, especially in the heated, shaken and pH-shift stressed samples.

**Intermolecular bonds and epitope integrity.** Sodium dodecyl sulfate PAGE (SDS-PAGE) was performed to elucidate whether the aggregates of stressed formulations were composed of covalently or non-covalently linked monomers. Dot blotting was used to verify epitope integrity of stressed formulations. The blots were probed with anti-heavy chain and anti-light chain antibodies (Fig. 4C and D).

**Sodium dodecyl sulfate PAGE (SDS-PAGE).** Under non-reducing conditions (Fig. 4A) all formulations showed a major band at around 150 kDa, which corresponds to the monomeric IgG. All formulations also showed thin bands with molecular weights smaller than the monomer band, indicating some degree of fragmentation, even in the unstressed sample, which however could be due to sample treatment. The oxidized sample lane contained a considerable amount of fragments and the monomer band was considerably fainter than the ones from other samples. The lane

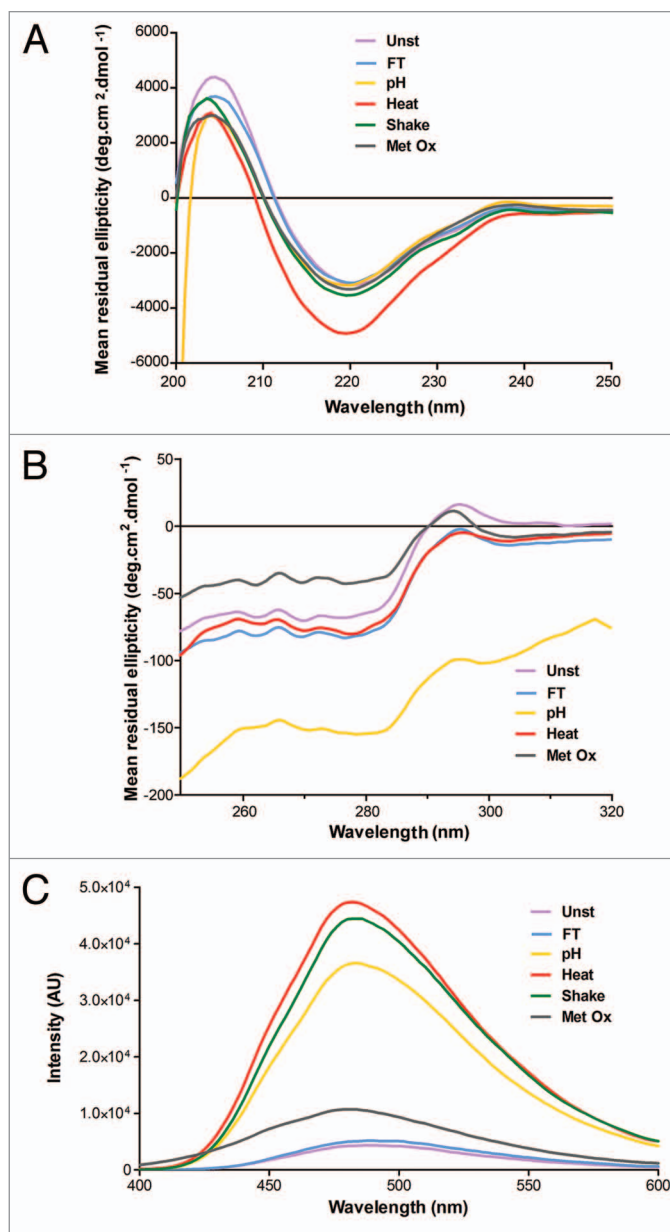


**Figure 3.** Structural characterization of unstressed (Unst), freeze-thawed (FT), pH-shifted (pH), heated (Heat), shaken (Shake) and metal-catalyzed oxidized (Metal Ox) IgG formulations by (A) far-UV CD, (B) near-UV CD and (C) Bis-ANS fluorescence.

of the oxidized sample had an overall darker tone than the ones of other samples for sizes below 250 kDa, suggesting the presence of fragments and small oligomers of monomers/fragments distributed throughout a wide range of molecular weights. Heated and shaken samples were the only ones containing a clear band on top of the gel. This indicates that these samples contained covalent aggregates that were too large to enter the gel.

Under reducing conditions (Fig. 4B), all formulations showed two main bands at ~50 and 25 kDa, deriving from the heavy and light chain. The unstressed, freeze-thawed, heated and shaken formulations showed also bands at 75, 125 and 150 kDa. These bands correspond to combinations of heavy and light chain

**Table 2.** Summary of physicochemical characteristics of unstressed and stressed IgG formulations

	Frag	Aggregates			Conform. changes		Hydroph	Covalent bonds	Epitope damage
		Olig	Submicron	Micron	Second	Tertiary			
Unst	-	-	-	-	-	-	-	-	-
FT	-	-	+	++	+	+	-	-	-
pH shift	-	++	++	+++	+	++	++	-	-
Heat	-	+++	+++	+	+	+	+++	++	-
Shake	-	-	+	+++	+	N/A	+++	++	-
Met Ox	++	+	+	+	+	++	+	-	-

Abbreviations: Unst, unstressed; FT, freeze-thawed; Met Ox, metal-catalyzed oxidized; Frag, fragments; Olig, oligomers; Conform, conformational; Second, secondary; Hydroph, hydrophobicity; N/A, not available (see text). Explanation of used symbols: negligible (-); mild (+); considerable (++); extensive (+++).

fragments, meaning that not all the disulfide bridges were broken. Interestingly, the pH-shift stressed did not contain these resistant fragments and the overall tone of the oxidized sample lane remained darker for sizes below 150 kDa than the tone of other lanes. The aggregated bands on top of the lanes of heated and shaken samples were no longer present under these conditions, indicating that they were covalently linked via disulfide bridges.

**Dot blotting.** The dot blots show that the antibodies were able to detect epitopes in both light and heavy chains. No clear differences were observed between the dots of the unstressed sample and all stressed samples, even at the lowest protein concentration. This indicates that all IgG samples contained intact epitopes after stress.

**Overall characterization.** The summary of the physicochemical characteristics of all stressed formulations can be found in Table 2.

**Immunogenicity.** The immunogenicity of the stressed formulations was tested by repeated injections in TG and NTG mice. These TG mice carry the human genes of Ig heavy and light chains, so they were expected to be more tolerant than the NTG mice to the human IgG administered in this study.<sup>29,37</sup> ADA titers were obtained by bridging ELISA from plasma collected before and during the injection period (6 weeks) and during a washout period of 10 weeks (Fig. 5).

**ADA titers.** Of all the mice administered with unstressed formulation, only one TG mouse responded by ADA formation (OD > 0.5). Because titers were too low to calculate, an arbitrary titer of 75 was given. This weak antibody response was transient and disappeared before the last week of the washout period, in contrast to the antibody responses to the stressed formulations, which were more persistent. Thus, the unstressed formulation was very poorly immunogenic and did not evoke a substantial antibody response in TG and NTG mice.

All stressed formulations induced an antibody response in at least 4 mice per total group (TG + NTG), with exception of the freeze-thawed formulation, which did not induce measurable ADAs in any mouse. Oxidized, heated and pH-shift stressed formulations were able to elicit an antibody response in both TG and NTG mice, whereas the shaken formulation only elicited the formation of ADAs in NTG mice. The groups administered with heated, shaken and pH-shift stressed formulations

had a relatively small number of responders per total group (4–6 out of 26 mice). On the other hand, an antibody response was observed in 19 out of 25 mice treated with the oxidized formulation. The ADAs induced by stressed formulations appeared 1 week before/after the last injection and most responders still had relatively high ADA titers during the last week of the washout period.

According to Mann-Whitney's test, the overall titers observed in NTG responders are significantly higher than the ones observed in TG responders (p value = 0.003). Further analysis revealed that only the NTG and TG mice treated with the oxidized formulation show significant differences in titers (p value = 0.045). The small number of responders in the other groups (i.e., low statistical power) likely contributes to the absence of significant difference in titers between NTG and TG mice, since the group with the second largest number of responders (pH-shift) showed nearly significant difference between TG and NTG titers (p = 0.079). In addition to statistical comparison of antibody titers, the McNemar's test was performed to assess a potential difference in number of responders between TG and NTG for all treatment groups together. Also here, no significant difference between the total number of TG and NTG responders was found (p value = 0.146).

## Discussion

The type of immune response that NTG mice develop against a human protein (classical immune response against a foreign protein) is expected to be different from the one developed by TG mice tolerant to this specific human protein (breaking/circumventing immune tolerance).<sup>38</sup> In fact, immunogenicity studies, involving the injection of either recombinant human insulin or recombinant human IFN $\alpha$  in NTG and immune tolerant TG mice, show that when practically aggregate-free formulations of these proteins were injected in NTG mice, most of them developed ADAs, whereas TG mice did not.<sup>6,37,39</sup> However, in our study, an immune reaction against unstressed human IgG in NTG mice was not observed. In fact, several studies have shown that the administration of aggregate-free foreign IgG can be very well tolerated in different animal species and in human patients, sometimes even when formulated in incomplete Freund's adjuvant or with lipopolysaccharides as adjuvants.<sup>40–44</sup>

The immunological mechanism of ADA induction to therapeutic proteins is not completely understood. Even though the presence of aggregates seems to play an important role on the development of ADAs, not all aggregates are equally immunogenic.<sup>5,6,37,45,46</sup> The stress methods used in this study induced different types of degraded IgG formulations. These contained different amounts of aggregates that varied in size distribution, type of intermolecular bonds, conformation, hydrophobicity and morphology. All formulations conserved intact epitopes after stress.

Freeze-thawing induced the lowest percentage of total aggregation (Table 1) and the lowest level of conformational changes (Fig. 3) compared with all other stressed methods. The aggregates of the freeze-thawed formulation were mostly micron-sized. In fact, this sample had the third highest amount of micron-sized aggregates of all stressed samples. The morphology of these aggregates was rather similar to the one of micron-sized aggregates of the oxidized formulation (Fig. 2). Even so, this sample was not able to induce a measurable antibody response in a single NTG or TG mouse. These results indicate that the micron-sized aggregates of this IgG, created by freeze-thawing cycles, are not immunogenic in these mice. They also suggest that the morphology of aggregates per se is not a good predictive feature for the immunogenicity of this IgG.

The pH-shift stressed formulation was heavily aggregated. This sample was characterized by having the most polydisperse set of aggregates, ranging from dimers to a few micrometers. This formulation induced rather low ADA titers in a relatively small amount of mice. Curiously, it elicited an immune response in more TG mice (31%) than in NTG mice (17%), even though this difference was not statically significant. These results indicate that aggregates induced by pH-shift stress increase the risk of immunogenicity of this IgG in these mice.

The heated formulation contained a large amount of oligomers and small submicron aggregates. This stress method induced pronounced structural changes and the formation of covalent aggregates. The antibody reaction to this sample was mild, with 23% of NTG and 8% of TG responders. Nevertheless, these results indicate that IgG aggregates induced by heat stress increase the risk of immunogenicity.

The shaken formulation exhibited the highest percentage of aggregates (88%) and contained mostly very large micron-sized aggregates. This sample was the only one containing visible precipitates. The micron-sized aggregates of this sample appeared to be fairly rounded and relatively dense under the microscope. At

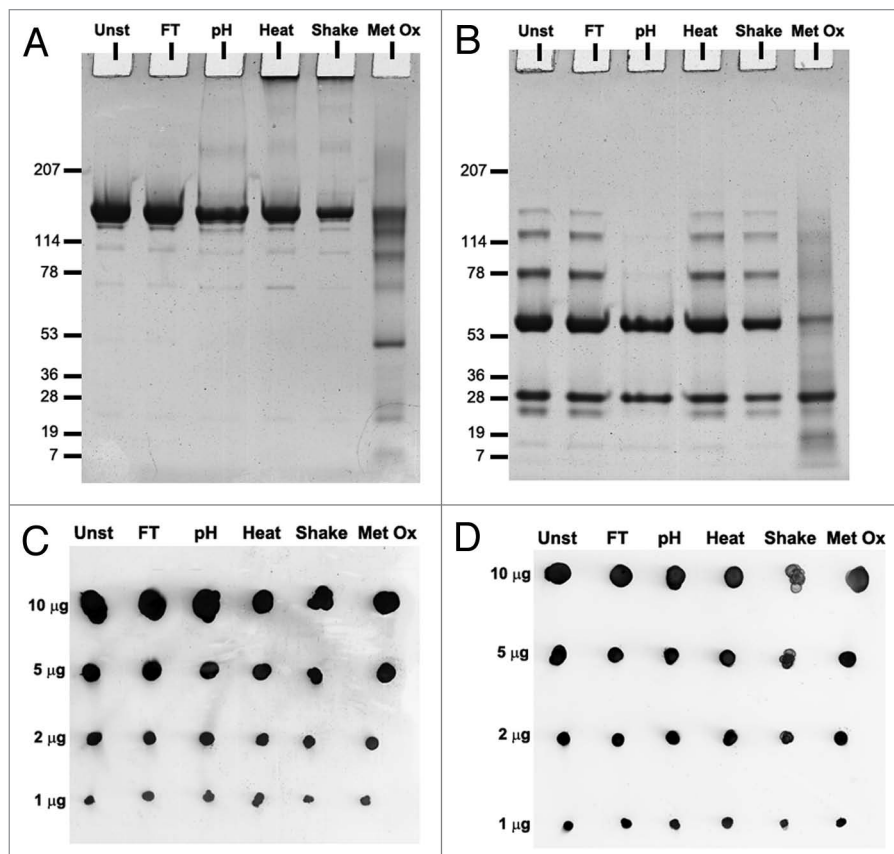


**Figure 4.** SDS-PAGE gels of unstressed (Unst), freeze-thawed (FT), pH-shifted (pH), heated (Heat), shaken (Shake) and metal-catalyzed oxidized (Metal Ox) IgG formulations stained with Coomassie brilliant blue under (A) non-reducing and (B) reducing conditions. Dot blots of the same formulations detected with (C) monoclonal anti-human  $\kappa$  light chain antibody (D) polyclonal anti-human heavy chain antibody.

least some of these aggregates were covalently linked. The extent of structural changes caused by this stress method could not be properly determined due to the interference of large aggregates. However, these changes are expected to be substantial, since this formulation showed one of the highest levels of bis-ANS fluorescence. Despite the great extent of aggregation and the large size of these aggregates, this formulation was only able to induce a measurable immune response in 31% of NTG mice and no ADA formation was observed in TG mice. These results indicate that aggregates induced by shake stress may only slightly increase the risk of immunogenicity.

The oxidized formulation was the one that elicited the strongest ADA response in the highest percentage of mice: 92% of NTG and 61% of TG mice. This result is consistent with the findings of other immunogenicity studies performed in NTG and TG mice, in which recombinant human IFN $\alpha$  and recombinant human IFN $\beta$  formulations stressed by metal-catalyzed oxidation revealed the highest immunogenic potential of a wide range of stressed formulations.<sup>37,46</sup> In our study, the oxidized IgG formulation was characterized by the following features: no visible aggregates, a small amount of subvisible aggregates, a large amount of fragments and fragment-derived oligomers, low hydrophobicity, elongated micron-sized aggregates with various

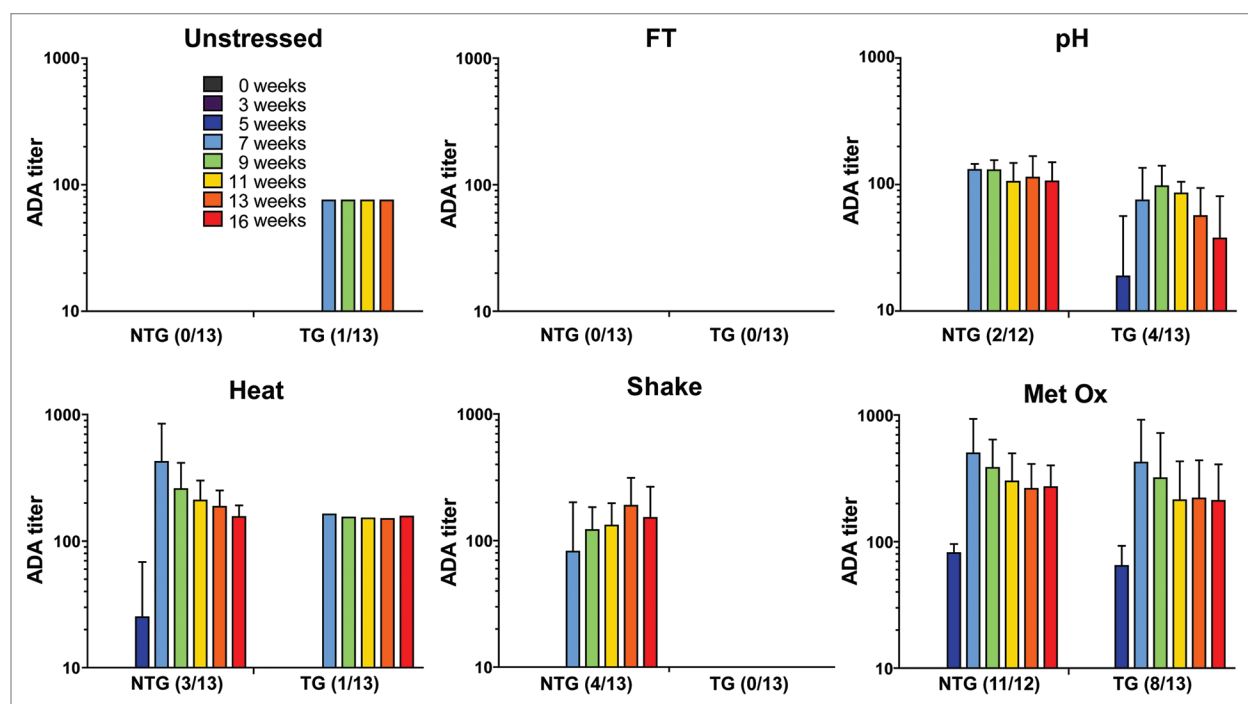


**Figure 5.** ADA titers of the sera of non-transgenic (NTG) and transgenic (TG) mice treated with unstressed (Unst), freeze-thawed (FT), pH-shifted (pH), heated (Heat), shaken (Shake) and metal-catalyzed oxidized (Metal Ox) human IgG formulations. Time points before the first injection (week 0), during the injection period (week 3 and 5) and after the last injection (week 7 to 16) are shown. The titers are from responders only and the error bars represent the standard deviation of the mean values.

shapes and densities, pronounced conformational changes and several chemical changes. Even though these features may give a hint about what may be relevant for immunogenicity of this IgG, the extreme heterogeneity of the aggregates present in this formulation make it impossible to pinpoint one specific species as the immunodominant one. For example, assuming that subvisible aggregates are not relevant for the immunogenicity of this IgG, based on the low amount detected in this sample, may be wrong. There is no evidence that rules out the possibility that this small amount of (metal-catalyzed oxidized) subvisible aggregates, or any other aggregate fraction, is sufficient to trigger a strong antibody response. Nevertheless, the results obtained in this study provide a strong indication that the quality of the IgG aggregates has more impact on the development of an immune response than their size or amount.

Injection of different purified fractions of aggregates could have helped to identify the immunodominant species, but protein aggregates are complex dynamic systems and the purification of a certain type of aggregate class without affecting the aggregation equilibrium is extremely difficult. Aggregates are very sensitive to any type of environmental changes and purification steps can actually be the starting point to the formation of more (and eventually different) aggregates.<sup>47</sup>

Metal-catalyzed oxidation of proteins is known to induce, among other modifications, the formation of mixed-disulfide derivatives and carbonyl derivatives of some amino acid residues, such as glutamyl semi-aldehyde, 2-amino-adipylsemialdehyde, pyroglutamyl and methionyl sulfoxide.<sup>48</sup> Reactive oxidized

protein species are involved in a wide range of biological pathways and, according to some immunological models, the presence of a significant amount of these oxidized species in the blood stream is considered a major danger signal for the immune system.<sup>49</sup> According to an immunogenicity study performed by Hermeling et al. involving the injection of degraded recombinant human IFN $\alpha$  in TG mice, oxidation per se is unlikely to be responsible for the high immunogenicity observed for oxidized formulations.<sup>37</sup> In our study, the oxidized IgG formulation contained a fair amount of aggregates, most likely formed by oxidized species, which indeed induced a high antibody response.

There was no statistically significant difference between the overall number of TG and NTG responders. However, the difference between ADA titers produced by TG and NTG responders was statistically significant: TG responders showed lower ADA titers. This was mostly due to the contribution of the group treated with oxidized formulation, and to a lesser extent to the other stressed IgG treated groups. This difference is not perceptible from the “Met Ox” graph of Figure 5, given that a logarithmic scale was used. However, ADA titers of NTG responders to the oxidized formulation were 24% higher than the ones produced by TG responders. This significant difference may indicate different immune reaction mechanisms between TG and NTG mice.

Previous publications on the five feature mouse model have shown that although Ig gene-rearrangements take place after antigen exposure, they are not as abundant compared with the rearrangements in non-transgenic control mice.<sup>31</sup> Also, they



indicate that the five feature mice have a lower percentage of B lymphocytes compared with non-transgenic mice. For this reason we investigated the antibody response against foreign proteins such as human serum albumin. In general, we observed that the five feature mice produce as much antibodies, and as fast, against these foreign proteins as non-transgenic control mice (data not shown). However, one should still consider the possibility that the immune response of these mice might be slightly compromised when testing other antigens. Moreover, these mice respond with mouse immune cells, so although relative immunogenicity might be predicted in these mice, our mouse model has its limitations.<sup>26</sup>

Overall, it is hard to draw a definitive conclusion about the advantage of using this specific TG mouse strain for assessing immunogenicity of human IgG compared with their NTG counterpart. Nevertheless, this study provides valuable information regarding the immunogenic potential of differently stressed IgG formulations.

### Conclusions

In this study, differently stressed IgG formulations were administered to TG and NTG mice, with the purpose of correlating the type and amount of aggregates with their immunogenic potential. In general, stress-induced aggregation of IgG leads to enhanced immunogenicity, but not all aggregates seem to pose the same immunogenic risk. The metal-catalyzed oxidized IgG formulation was the most immunogenic. The presence of oxidized IgG species, probably incorporated in aggregates, has more impact on the immunogenicity of this IgG than any other aggregate feature investigated in this work: size, amount, structural conformation, hydrophobicity, morphology and type of intermolecular bonds.

For the first time, the risk of different types and amounts of degraded IgG, in particular aggregates, on immunogenicity has been studied in transgenic mice containing human Ig genes. This study provided useful insights on IgG aggregate-related immunogenicity, but clearly more research is needed to be able to determine the immunogenic potential of different types and amounts of IgG aggregates and other degradation products.

### Materials and Methods

**Materials.** A non-marketed recombinant fully human monoclonal antibody of the IgG1 subclass was used for this experiment at an initial concentration of 0.5 mg/ml. The buffer used to formulate and dilute the IgG contained 10 mM sodium citrate (Merck), 5% (w/v) sucrose (Sigma-Aldrich), pH 6.0. The buffer was filtered using a 0.22- $\mu$ m PES low binding syringe-driven filter unit (Millex™ GP, Millipore). Sodium phosphate, sodium sulfate, sodium azide, copper chloride, ascorbic acid, EDTA (EDTA), hydrochloric acid (HCl), acetic acid, tris(hydroxymethyl)aminomethane (Tris), TRIS-HCl, glycine, sodium dodecyl sulfate (SDS) and Tween 20 were purchased from Sigma-Aldrich, sodium hydroxide (NaOH) from Boom BV, methanol from Biosolve BV and the fluorescent dye

4,4'-dianilino-1,1'-binaphthyl-5,5'-disulfonic acid dipotassium salt (bis-ANS) from Fluka.

**IgG stressing procedures.** The IgG formulation (0.5 mg/ml) was stressed by five different accelerated stress methods to create aggregates. Freeze-thawing stress was performed by applying 10 cycles of incubation of 1 ml of IgG solution in 1.5-ml reaction tubes (Eppendorf) at  $-80^{\circ}\text{C}$  for 20 min followed by incubation at room temperature (RT) for 20 min. The pH-shift stress consisted of changing 3 times the formulation buffer pH from pH 6 to pH 1 and back to pH 6 at RT. NaOH (5 M) and HCl (5 M) were alternatively added drop wise to induce the pH-shifts. Each cycle consisted in approximately 1 min exposure to pH 1. The heat stress was performed by incubating 1 ml of IgG solution in 1.5-ml reaction tubes at  $74^{\circ}\text{C}$  for 15 min in an Eppendorf Thermomixer® R. The shake stress was done in an IKA KS 4000i control shaker (IKA WORKS) and consisted of placing 1 ml of IgG solution in 2-ml reaction tubes (Eppendorf) and shaking them with orbital agitation at 400 rpm for 16 h at RT. The tubes were placed horizontally in the shaker to increase the turbulence inside. The metal-catalyzed oxidation was achieved by incubating IgG solution with 8 mM ascorbic acid and 0.08 mM  $\text{CuCl}_2$  for 3 h at RT, according to Li et al.<sup>50</sup> The reaction was stopped by adding EDTA (100 mM) to a final concentration of 1 mM. This sample was dialyzed extensively against formulation buffer with a 3.5 kDa MWCO Slide-A-Lyzer Cassette (Perbio Science). The samples for injections were diluted 10-fold and stored at  $4^{\circ}\text{C}$  for 3 d, until their administration to mice. The samples used for analysis are the physical mixture of 8 individually stressed samples (1 ml each) and stored at  $4^{\circ}\text{C}$  for 2–3 d, until analysis.

**Size-exclusion chromatography (SEC).** SEC was performed on an Agilent 1200 (Agilent Technologies) combined with a Wyatt Eclipse (Wyatt Technology Europe GmbH). A TSK Gel 4000  $\text{SW}_{\text{XL}}$  column (300 mm  $\times$  7.8 mm) with a TSK Gel 4000  $\text{SW}_{\text{XL}}$  pre-column (Tosoh Bioscience) was used. 100  $\mu\text{L}$  of each formulation was injected and separation was performed at a flow rate of 0.5 ml/min. The elution buffer was composed of 100 mM sodium phosphate, 100 mM sodium sulfate, 0.05% (w/v) sodium azide at pH 7.1. UV detection was performed at 280 nm with the Agilent 1200 apparatus, whereas multiple angle laser light scattering (MALLS) detection was performed with an 18-angle DAWN HELEOS™ detector (Wyatt Technology Europe) operating with a 50-nW solid-state laser at 658 nm. The molecular weight of the IgG peaks was calculated with the Astra software version 5.3.1.5 (Wyatt Technology Europe). An extinction coefficient of 1.69 ( $\text{ml mg}^{-1} \text{cm}^{-1}$ ), a  $\text{dn/dc}$  of 0.185 ( $\text{ml/g}$ ) and a second virial coefficient of 0 were used. The calculation of the molecular weight was based on the Zimm equation.<sup>51</sup>

The AUC of the UV signal was used to calculate the percentage of fragments, monomers, oligomers, protein recovery and total aggregation. For the relative protein recovery, the total AUC of the stressed samples was compared with the total AUC of the unstressed sample, which was set to 100%. Total aggregation percentages take into account not only the AUC of the oligomers but also the percentage of protein not recovered, which normally comprises aggregates that are too big to enter the column.

**Nanoparticle tracking analysis (NTA).** NTA measurements were performed with a NanoSight LM20 (NanoSight), equipped with a sample chamber with a 640-nm laser and a Viton fluoro-elastomer O-ring, as described previously.<sup>17</sup> Briefly, the samples were injected in the sample chamber with sterile BD Discardit II syringes (Becton, Dickinson and Company) until the liquid reached the tip of the nozzle and measurements were taken at 27°C with a viscosity of 0.89 centipoise. The buffer viscosity was measured in an AR-G2 rheometer from TA Instruments. The NTA 2.1 software was used for capturing and analyzing the data. The samples were measured for 40 sec with manual shutter and gain adjustments. At least six measurements of each sample were performed and the mean was obtained. The heat stressed sample was diluted 20 times before measurements, whereas the pH-shift stressed sample was diluted 10 times and required the use of the extended dynamic range mode due to the high polydispersity observed. Final counts were adjusted based on the dilution factor.

**Light obscuration (LO).** LO measurements were performed on a PAMAS SVSS system (PAMAS GmbH) equipped with a HCB-LD-25/25 sensor and a 1-ml syringe. Each sample was measured three times, with each measurement consisting of a pre-run volume of 0.3 ml followed by three runs of 0.2 ml at a flow rate of 10 ml/min. The final results are a mean of the three runs and the error bars represent the standard deviation between them. The shake stressed sample was diluted 4 times before measurements and the final counts were adjusted.

**Filtration with Coomassie Blue staining.** A volume of 3 ml of ultrapure (Milli-Q) water was filtered through 0.22- $\mu$ m PES syringe-driven filter units of 13 mm from Millipore, to wash out any particulate matter that could have been present in the membrane. Then 1.5 ml of each IgG sample was filtered through these filters, with exception of the shake stress sample, from which only 150  $\mu$ l were used, due to membrane blocking issues. The membranes were incubated with Coomassie brilliant blue R-250 (Biorad) in 45% (v/v) methanol (Biosolve BV) and 10% (v/v) acetic acid for 10 min. The membranes were then destained with a solution containing 10% (v/v) methanol and 10% (v/v) acetic acid for 3 h. The membranes were analyzed with an Axioskop microscope (Carl Zeiss), using a 20 $\times$  amplification objective. Images were collected randomly using the ProgRes CapturePro v2.8.8 software (Jenoptik AG).

**Visual inspection.** Stressed samples were inspected visually, inside reaction tubes, for the presence of visible particles. Formulation buffer (transparent and uncolored) was used as a reference.

**Circular dichroism (CD).** CD was performed with a Jasco J-815 CD spectrometer in combination with a Jasco PTC-423S temperature controller (Jasco International) at 25°C. The samples were diluted to 0.1 mg/ml for far-UV CD and kept at 0.5 mg/ml for near-UV CD measurements. The shake-stressed sample was centrifuged at 10,000 rpm for 1 min and the supernatant was used undiluted for far-UV CD measurements. The samples were measured in quartz cuvettes (Hellma GmbH) with a path length of 1 mm for far-UV CD and 10 mm for near-UV CD. CD spectra were collected in a continuous scanning method from 200 to 250 nm for far-UV CD and from 250 to 320 nm for

near-UV CD. The measurements were performed at a scanning speed of 50 nm/min, a response time of 2 sec, a bandwidth of 1 nm, a sensitivity of 100 m $^{\circ}$ , steps of 0.5 nm and an accumulation of 10 scans. Using the Spectra Analysis Software (version 1.53.04, Jasco), the spectra were background-corrected by subtracting the spectrum of the buffer and smoothed with GraphPad Prism<sup>®</sup> 5 (GraphPad Software) with a 0th order polynomial smoothing and 4 neighbors on each value. Data were calculated as mean residue ellipticity according to Kelly et al.,<sup>32</sup> using a mean amino acid residue weight of 113 suggested by Aghaie et al.<sup>52</sup> for IgG.

**Steady-state fluorescence spectroscopy.** Steady-state fluorescence was measured with a Tecan Infinite M1000 plate reader (Tecan Benelux) with 96-well plates (Greiner Bio-One), a sample volume of 200  $\mu$ l per well (n = 3), a gain of 189 and a Z-position of 21500  $\mu$ m. Bis-ANS was added to the wells to a final concentration of 1  $\mu$ M. The samples were excited at 385 nm and the emission spectra were recorded from 400 nm to 600 nm. The spectra of the 3 wells were averaged and the average was then smoothed in the GraphPad Prism<sup>®</sup> 5 software with a 0th order polynomial smoothing and 4 neighbors on each value.

**Sodium dodecyl sulfate PAGE (SDS-PAGE).** SDS-PAGE was performed with a Biorad Mini-Protean 3 module (Bio-Rad).<sup>25</sup> Briefly, 11  $\mu$ g of protein were loaded in 4–20% linear gradient TRIS-HCl Ready Gels from Bio-Rad and the gels were run under non-reducing and reducing (sample buffer containing 5% (v/v)  $\beta$ -mercaptoethanol from Sigma Aldrich) conditions at 100 V and at RT. The bands were detected by Coomassie brilliant blue R-250 staining and the gels were scanned with a Bio-Rad GS-800 densitometer and Quantity One software.

**Dot blotting.** For dot blotting analysis, different volumes of each IgG sample (0.5 mg/ml) were spotted two nitrocellulose membranes (VWR International) to make up a total protein amount of 10, 5, 2 and 1  $\mu$ g per spot. The blots were blocked for 1 h at RT with 5% (w/v) non-fat milk powder (ELK, Campina Melkunie) in TBS-T<sub>0.05</sub> (50 mM TRIS-HCl, 150 mM sodium chloride and 0.05% (w/v) Tween 20, pH 7.4) with constant orbital shaking. After washing with TBS-T<sub>0.05</sub>, the blots were probed overnight at 4°C with primary antibodies in milk solution as follows: anti-human Ig  $\kappa$  light chain constant region antibody (rabbit monoclonal IgG, 1:1000, Abcam) and anti-human IgG<sub>1</sub> heavy chain constant region antibody (mouse polyclonal IgG, 1:2000, Abcam). The blots were washed with TBS-T<sub>0.05</sub> and probed for 1 h at RT with appropriate secondary antibodies in milk solution as follows: anti-rabbit IgG (goat polyclonal IgG, horse radish peroxidase (HRP) labeled, 1:2000, Jackson ImmunoResearch) and anti-mouse IgG (goat polyclonal IgG, HRP labeled, 1:2000, Jackson ImmunoResearch). Afterwards, the blots were washed with TBS-T<sub>0.05</sub> and incubated with ECL Plus reagent (GE Healthcare) for 2 min and detected with a Typhoon 9400 fluorescence imager (GE Healthcare).

**Mouse Strain.** Five feature mice developed at the Babraham Institute carry the human Ig heavy and both  $\kappa$ - and  $\lambda$ -light chain transloci in a background in which the endogenous heavy and  $\kappa$ -light loci have been inactivated. As a result they have basal expression of human IgM, Ig $\kappa$  and Ig $\lambda$  and are capable of forming a large human antibody repertoire involving translocus

rearrangement and somatic hypermutation.<sup>31</sup> This strongly suggests that these mice are capable of forming isotype switched antibodies (such as IgG) upon exposure to an antigen, but this has not been investigated yet. These mice were originally developed to produce therapeutic human mAbs of desired specificities, but their endogenous expression of human antibodies may also render them a good model to study immunogenicity of human mAbs. Non-transgenic (NTG) mice were used as a control in our experiment. These mice are from the same breeding stock as five-feature translocus mice, but lost the human genes along the breeding process.

**Breeding and genotyping.** Frozen five feature embryos were transported from the Babraham Institute to the local animal housing facility at the Utrecht University, where they were implanted in pseudo pregnant females. Pups were genotyped for TG state (see supplemental data), and used to set up a stable TG mouse line. To obtain both TG mice and their NTG littermates for the experiments, breeding was performed by crossing a heterozygote TG male with a heterozygote TG female. This breeding scheme ensured transfer of all transgenes to the offspring, although still a significant number of NTG littermates were born. The TG state of the offspring was determined by isolating in chromosomal DNA isolated from ear tissue and subsequent PCR to determine the presence of the human heavy chain and human  $\lambda$  and  $\kappa$  light chains (see supplemental data for primers). Absence of mouse heavy and  $\kappa$  light chains was of less importance to the study and therefore not tested.

**Animal experiment.** A total of 78 TG mice and 78 NTG littermates (females and males, 10–14 weeks of age at the start of the experiment) were included in the study. All mice had free access to food (Hope Farms) and water (acidified).

TG mice and NTG littermates ( $n = 13$ ) were treated with unstressed IgG formulation, or 1 out of 5 stressed IgG formulations, once per week for 6 weeks (intraperitoneal injections, 5  $\mu\text{g}$  protein/injection). The interval between injections was 1 week. The formulations were mildly vortexed before injections to prevent aggregate deposition in the tubes. Blood was collected submandibularly from all mice before treatment was started (week 0), during the 6 week injection period (before injections on weeks 3 and 5), and during a 7 week washout phase (weeks 7, 9, 11 and 13). At 10 weeks after the last injection (week 16) blood was collected by heart puncture and mice were sacrificed. Blood was collected in Lithium-heparin gel tubes and spun down (3000 g, 10 min, 4°C) to isolate the plasma. Plasma was stored at -80°C until analysis.

**ADA assay.** To test plasma samples for ADAs against the injected IgG, a bridging ELISA was used. This assay setup focuses on binding antibodies and does not allow determination of the isotype of the measured response. This type of ELISA is very commonly used in clinics to determine antibody

responses against therapeutic mAbs because of its high sensitivity and reproducibility and because it does not require the use of radioactive compounds. In short, 96-well F-bottom ELISA-plates (Greiner Bio-One) were coated with 0.5  $\mu\text{g}/\text{ml}$  of unstressed IgG in phosphate buffered saline (PBS) and stored overnight at 4°C. Prior to use, the plates were washed five times with PBS containing 0.05% (w/v) of Tween-20 (PBS-T<sub>0.05</sub>), and incubated for 1 h at RT with plasma samples serially diluted (starting dilution 1:100) in high performance ELISA buffer (HPE, Business Unit Reagents). Subsequent to washing with PBS-T<sub>0.05</sub>, the plates were incubated for 1 h at RT with 1  $\mu\text{g}/\text{ml}$  of unstressed IgG biotinylated in HPE buffer (biotinylation of the drug was adapted from Van Schouwenburg et al.<sup>53</sup>). After washing with PBS-T<sub>0.05</sub>, the plates were incubated for 20 min at RT with 1:10000 of Avidin-HRP (Invitrogen) in HPE buffer. The plates were then washed with PBS-T<sub>0.05</sub> and developed with TMB substrate (Invitrogen) for 15 min. The development was stopped by adding 0.18 M of H<sub>2</sub>SO<sub>4</sub>. Absorbance was measured at 405 nm (SpectroStar Nano, Isogen). The 100-fold diluted plasma samples were arbitrarily defined positive if their optical density (OD) was at least 0.5 higher than the negative control. ADA titers were determined by plotting the absorbance values of the dilution series against log dilution. The plots were fitted to a sigmoidal dose-response curve using GraphPad Prism® 4. The reciprocal of the dilution of the EC<sub>50</sub> value was defined as the ADA titer. Plasma samples considered positive (OD > 0.5) but having too low OD for assessing titers via EC<sub>50</sub> (OD ~1.45) were given an arbitrary titer of 75.

**Statistics.** Using the SPSS software v. Sixteen (Microsoft), a non-parametric Mann-Whitney U test was used to assess the statistical difference in titers between TG and NTG responders. Significant difference in the number of responders between groups was determined with the McNemar's test. A calculated probability (p value) equal or below 0.05 was considered to be statistically significant.

#### Disclosure of Potential Conflicts of Interest

No potential conflicts of interest were disclosed.

#### Acknowledgments

This research was supported by the Technology Foundation STW, the applied science division of NWO and technology program of the Dutch Ministry of Economic Affairs. This experiment was approved by the Institutional Ethical Committee (Utrecht University). The authors would like to acknowledge Diana Wouters and Lucien Aarden for their support with setting up the ADA assays.

#### Supplemental Material

Supplemental material may be found here:  
[www.landesbioscience.com/journals/mabs/article/22066](http://www.landesbioscience.com/journals/mabs/article/22066)

#### References

1. Lawrence S. Pipelines turn to biotech. *Nat Biotechnol* 2007; 25:1342; PMID:18066015; <http://dx.doi.org/10.1038/nbt1207-1342>
2. Bartelds GM, Kriekaert CL, Nurmohamed MT, van Schouwenburg PA, Lems WF, Twisk JW, et al. Development of antidrug antibodies against adalimumab and association with disease activity and treatment failure during long-term follow-up. *JAMA* 2011; 305:1460-8; PMID:21486979; <http://dx.doi.org/10.1001/jama.2011.406>
3. Bartelds GM, Wijbrandts CA, Nurmohamed MT, Stapel S, Lems WF, Aarden L, et al. Clinical response to adalimumab: relationship to anti-adalimumab antibodies and serum adalimumab concentrations in rheumatoid arthritis. *Ann Rheum Dis* 2007; 66:921-6; PMID:17301106; <http://dx.doi.org/10.1136/ard.2006.065615>



4. Schellekens H. Bioequivalence and the immunogenicity of biopharmaceuticals. *Nat Rev Drug Discov* 2002; 1:457-62; PMID:12119747; <http://dx.doi.org/10.1038/nrd818>
5. Rosenberg AS. Effects of protein aggregates: an immunologic perspective. *AAPS J* 2006; 8:E501-7; PMID:17025268; <http://dx.doi.org/10.1208/aapsj080359>
6. Braun A, Kwee L, Labow MA, Alsenz J. Protein aggregates seem to play a key role among the parameters influencing the antigenicity of interferon alpha (IFN-alpha) in normal and transgenic mice. *Pharm Res* 1997; 14:1472-8; PMID:9358564; <http://dx.doi.org/10.1023/A:1012193326789>
7. Gamble CN. The role of soluble aggregates in the primary immune response of mice to human gamma globulin. *Int Arch Allergy Appl Immunol* 1966; 30:446-55; PMID:4163860; <http://dx.doi.org/10.1159/000229829>
8. Cheng PC, Steele CR, Gu L, Song W, Pierce SK. MHC class II antigen processing in B cells: accelerated intracellular targeting of antigens. *J Immunol* 1999; 162:7171-80; PMID:10358163
9. Daha MR, van ES LA, Hazvoet HM, Kijlstra A. Degradation of soluble immunoglobulin aggregates in vitro by monocytes from normal subjects and from patients with systemic lupus erythematosus. *Scand J Immunol* 1982; 16:117-22; PMID:7134889; <http://dx.doi.org/10.1111/j.1365-3083.1982.tb00705.x>
10. Johnson R, Jiskoot W. Models for evaluation of relative immunogenic potential of protein particles in biopharmaceutical protein formulations. *J Pharm Sci* 2012; 101:3586-92; PMID:22736238; <http://dx.doi.org/10.1002/jps.23248>
11. Filipe V, Hawe A, Schellekens H, Jiskoot W. Aggregation and immunogenicity of therapeutic proteins. In: Wang W, Roberts CJ, eds. *Aggregation of therapeutic proteins*. New Jersey: John Wiley & Sons, 2010:403-33
12. Mahler HC, Friess W, Grauschopf U, Kiese S. Protein aggregation: pathways, induction factors and analysis. *J Pharm Sci* 2009; 98:2909-34; PMID:18823031; <http://dx.doi.org/10.1002/jps.21566>
13. den Engelsman J, Garidel P, Smulders R, Koll H, Smith B, Bassarab S, et al. Strategies for the assessment of protein aggregates in pharmaceutical biotech product development. *Pharm Res* 2011; 28:920-33; PMID:20972611; <http://dx.doi.org/10.1007/s11095-010-0297-1>
14. Carpenter JF, Randolph TW, Jiskoot W, Crommelin DJ, Middaugh CR, Winter G, et al. Overlooking subvisible particles in therapeutic protein products: gaps that may compromise product quality. *J Pharm Sci* 2009; 98:1201-5; PMID:18704929; <http://dx.doi.org/10.1002/jps.21530>
15. Singh SK, Afonina N, Awwad M, Bechtold-Peters K, Blue JT, Chou D, et al. An industry perspective on the monitoring of subvisible particles as a quality attribute for protein therapeutics. *J Pharm Sci* 2010; 99:3302-21; PMID:20310025; <http://dx.doi.org/10.1002/jps.22097>
16. Hawe A, Hulse WL, Jiskoot W, Forbes RT. Taylor dispersion analysis compared to dynamic light scattering for the size analysis of therapeutic peptides and proteins and their aggregates. *Pharm Res* 2011; 28:2302-10; PMID:21560019; <http://dx.doi.org/10.1007/s11095-011-0460-3>
17. Filipe V, Hawe A, Jiskoot W. Critical evaluation of Nanoparticle Tracking Analysis (NTA) by NanoSight for the measurement of nanoparticles and protein aggregates. *Pharm Res* 2010; 27:796-810; PMID:20204471; <http://dx.doi.org/10.1007/s11095-010-0073-2>
18. Barnard JG, Singh S, Randolph TW, Carpenter JF. Subvisible particle counting provides a sensitive method of detecting and quantifying aggregation of monoclonal antibody caused by freeze-thawing: insights into the roles of particles in the protein aggregation pathway. *J Pharm Sci* 2011; 100:492-503; PMID:20803602; <http://dx.doi.org/10.1002/jps.22305>
19. Wuchner K, Büchler J, Spycher R, Dalmonte P, Volkin DB. Development of a microflow digital imaging assay to characterize protein particulates during storage of a high concentration IgG1 monoclonal antibody formulation. *J Pharm Sci* 2010; 99:3343-61; PMID:20229596; <http://dx.doi.org/10.1002/jps.22123>
20. Barnard JG, Rhyner MN, Carpenter JF. Critical evaluation and guidance for using the Coulter method for counting subvisible particles in protein solutions. *J Pharm Sci* 2012; 101:140-53; PMID:22109687; <http://dx.doi.org/10.1002/jps.22732>
21. De Groot AS, McMurry J, Moise L. Prediction of immunogenicity: in silico paradigms, ex vivo and in vivo correlates. *Curr Opin Pharmacol* 2008; 8:620-6; PMID:18775515; <http://dx.doi.org/10.1016/j.coph.2008.08.002>
22. Wullner D, Zhou L, Bramhall E, Kuck A, Goletz TJ, Swanson S, et al. Considerations for optimization and validation of an in vitro PBMC derived T cell assay for immunogenicity prediction of biotherapeutics. *Clin Immunol* 2010; 137:5-14; PMID:20708973; <http://dx.doi.org/10.1016/j.clim.2010.06.018>
23. Joubert MK, Hokom M, Eakin C, Zhou L, Deshpande M, Baker MP, et al. Highly Aggregated Antibody Therapeutics Can Enhance the In Vitro Innate and Late-stage T-cell Immune Responses. *J Biol Chem* 2012; 287:25266-79; PMID:22584577; <http://dx.doi.org/10.1074/jbc.M111.330902>
24. Hermeling S, Schellekens H, Maas C, Gebbink MF, Crommelin DJ, Jiskoot W. Antibody response to aggregated human interferon alpha2b in wild-type and transgenic immune tolerant mice depends on type and level of aggregation. *J Pharm Sci* 2006; 95:1084-96; PMID:16552750; <http://dx.doi.org/10.1002/jps.20599>
25. van Beers MM, Sauerborn M, Gilli F, Brinks V, Schellekens H, Jiskoot W. Aggregated recombinant human interferon Beta induces antibodies but no memory in immune-tolerant transgenic mice. *Pharm Res* 2010; 27:1812-24; PMID:20499141; <http://dx.doi.org/10.1007/s11095-010-0172-0>
26. Brinks V, Jiskoot W, Schellekens H. Immunogenicity of therapeutic proteins: the use of animal models. *Pharm Res* 2011; 28:2379-85; PMID:21744171; <http://dx.doi.org/10.1007/s11095-011-0523-5>
27. Schellekens H. How to predict and prevent the immunogenicity of therapeutic proteins. *Biotechnol Annu Rev* 2008; 14:191-202; PMID:18606364; [http://dx.doi.org/10.1016/S1387-2656\(08\)00007-0](http://dx.doi.org/10.1016/S1387-2656(08)00007-0)
28. van Beers MM, Sauerborn M, Gilli F, Hermeling S, Brinks V, Schellekens H, et al. Hybrid transgenic immune tolerant mouse model for assessing the breaking of B cell tolerance by human interferon beta. *J Immunol Methods* 2010; 352:32-7; PMID:19857496; <http://dx.doi.org/10.1016/j.jim.2009.10.005>
29. Hermeling S, Jiskoot W, Crommelin D, Bornaes C, Schellekens H. Development of a transgenic mouse model immune tolerant for human interferon Beta. *Pharm Res* 2005; 22:847-51; PMID:15948027; <http://dx.doi.org/10.1007/s11095-005-4578-z>
30. Hermeling S, Schellekens H, Maas C, Gebbink MF, Crommelin DJ, Jiskoot W. Antibody response to aggregated human interferon alpha2b in wild-type and transgenic immune tolerant mice depends on type and level of aggregation. *J Pharm Sci* 2006; 95:1084-96; PMID:16552750; <http://dx.doi.org/10.1002/jps.20599>
31. Nicholson IC, Zou X, Popov AV, Cook GP, Corps EM, Humphries S, et al. Antibody repertoires of four- and five-feature translocus mice carrying human immunoglobulin heavy chain and kappa and lambda light chain yeast artificial chromosomes. *J Immunol* 1999; 163:6898-906; PMID:10586092
32. Kelly SM, Jess TJ, Price NC. How to study proteins by circular dichroism. *Biochim Biophys Acta* 2005; 1751:119-39; PMID:16027053; <http://dx.doi.org/10.1016/j.bbapap.2005.06.005>
33. Hawe A, Sutter M, Jiskoot W. Extrinsic fluorescent dyes as tools for protein characterization. *Pharm Res* 2008; 25:1487-99; PMID:18172579; <http://dx.doi.org/10.1007/s11095-007-9516-9>
34. Demeule B, Lawrence MJ, Drake AF, Gurny R, Arvinte T. Characterization of protein aggregation: the case of a therapeutic immunoglobulin. *Biochim Biophys Acta* 2007; 1774:146-53; PMID:17142116; <http://dx.doi.org/10.1016/j.bbapap.2006.10.010>
35. Pelton JT, McLean LR. Spectroscopic methods for analysis of protein secondary structure. *Anal Biochem* 2000; 277:167-76; PMID:10625503; <http://dx.doi.org/10.1006/abio.1999.4320>
36. Imanishi A, Isemura T. Circular dichroic spectra of L-cystine and its dihydrochloride crystals in KBr disc in relation to the circular dichroism of disulfide bonds in proteins. *J Biochem* 1969; 65:309-12; PMID:5711957
37. Hermeling S, Aranha L, Damen JM, Slijper M, Schellekens H, Crommelin DJ, et al. Structural characterization and immunogenicity in wild-type and immune tolerant mice of degraded recombinant human interferon alpha2b. *Pharm Res* 2005; 22:1997-2006; PMID:16184451; <http://dx.doi.org/10.1007/s11095-005-8177-9>
38. Schellekens H. Immunogenicity of therapeutic proteins. *Nephrology, dialysis, transplantation: official publication of the European Dialysis and Transplant Association. European Renal Association* 2003; 18:1257-9
39. Ottesen JL, Nilsson P, Jami J, Weiglun D, Dührkop M, Bucchini D, et al. The potential immunogenicity of human insulin and insulin analogues evaluated in a transgenic mouse model. *Diabetologia* 1994; 37:1178-85; PMID:7895946; <http://dx.doi.org/10.1007/BF00399790>
40. Weksler ME, Bull G, Schwartz GH, Stenzel KH, Rubin AL. Immunologic responses of graft recipients to antilymphocyte globulin: effect of prior treatment with aggregate-free gamma globulin. *J Clin Invest* 1970; 49:1589-95; PMID:4194090; <http://dx.doi.org/10.1172/JCI106376>
41. Cerottini JC, Lambert PH, Dixon FJ. Comparison of the immune responsiveness of NZB and NZB X NZW F1 hybrid mice with that of other strains of mice. *J Exp Med* 1969; 130:1093-105; PMID:4186796; <http://dx.doi.org/10.1084/jem.130.5.1093>
42. Biro CE, Garcia G. The Antigenicity of Aggregated and Aggregate-Free Human Gamma-Globulin for Rabbits. *Immunology* 1965; 8:411-9; PMID:14279046
43. Golub ES, Weigle WO. Studies on the induction of immunologic unresponsiveness. 3. Antigen form and mouse strain variation. *J Immunol* 1969; 102:389-96; PMID:4179469
44. Fujiwara M, Fujiwara S, Yoshizaki C, Awaya A. Strain differences in the immunogenicity of aggregated human IgG and the adjuvant action of lipopolysaccharide on the low-responder strain of mice. *Jpn J Microbiol* 1976; 20:141-6; PMID:781351
45. Moore WV, Leppert P. Role of aggregated human growth hormone (hGH) in development of antibodies to hGH. *J Clin Endocrinol Metab* 1980; 51:691-7; PMID:7419661; <http://dx.doi.org/10.1210/jcem-51-4-691>
46. van Beers MM, Sauerborn M, Gilli F, Brinks V, Schellekens H, Jiskoot W. Oxidized and aggregated recombinant human interferon beta is immunogenic in human interferon beta transgenic mice. *Pharm Res* 2011; 28:2393-402; PMID:21544687; <http://dx.doi.org/10.1007/s11095-011-0451-4>
47. Philo JS. Is any measurement method optimal for all aggregate sizes and types? *AAPS J* 2006; 8:E564-71; PMID:17025274; <http://dx.doi.org/10.1208/aapsj080365>
48. Stadman ER. Metal ion-catalyzed oxidation of proteins: biochemical mechanism and biological consequences. *Free Radic Biol Med* 1990; 9:315-25; PMID:2283087; [http://dx.doi.org/10.1016/0891-5849\(90\)90006-5](http://dx.doi.org/10.1016/0891-5849(90)90006-5)



49. Gallucci S, Matzinger P. Danger signals: SOS to the immune system. *Curr Opin Immunol* 2001; 13:114-9; PMID:11154927; [http://dx.doi.org/10.1016/S0952-7915\(00\)00191-6](http://dx.doi.org/10.1016/S0952-7915(00)00191-6)
50. Li S, Nguyen TH, Schöneich C, Borchardt RT. Aggregation and precipitation of human relaxin induced by metal-catalyzed oxidation. *Biochemistry* 1995; 34:5762-72; PMID:7727437; <http://dx.doi.org/10.1021/bi00017a008>
51. Zimm BH. The dependence of the scattering of light on angle and concentration in linear polymer solutions. *J Phys Colloid Chem* 1948; 52:260-7; PMID:18918874; <http://dx.doi.org/10.1021/j150457a022>
52. Aghaie A, Pourfathollah AA, Bathaie SZ, Moazzeni SM, Pour HK, Banazadeh S. Structural study on immunoglobulin G solution after pasteurization with and without stabilizer. *Transfus Med* 2008; 18:62-70; PMID:18279194; <http://dx.doi.org/10.1111/j.1365-3148.2007.00778.x>
53. van Schouwenburg PA, Bartelds GM, Hart MH, Aarden L, Wolbink GJ, Wouters D. A novel method for the detection of antibodies to adalimumab in the presence of drug reveals "hidden" immunogenicity in rheumatoid arthritis patients. *J Immunol Methods* 2010; 362:82-8; PMID:20833178; <http://dx.doi.org/10.1016/j.jim.2010.09.005>